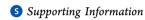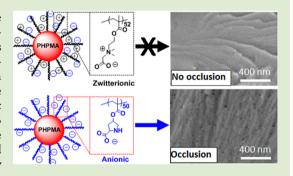# Incorporating Diblock Copolymer Nanoparticles into Calcite Crystals: Do Anionic Carboxylate Groups Alone Ensure Efficient Occlusion?

Yin Ning,[†] Lee A. Fielding,[†,‡] Kay E. B. Doncom,[†] Nicholas J. W. Penfold,[†] Alexander N. Kulak,[§] Hideki Matsuoka,[∥] and Steven P. Armes*,[†]

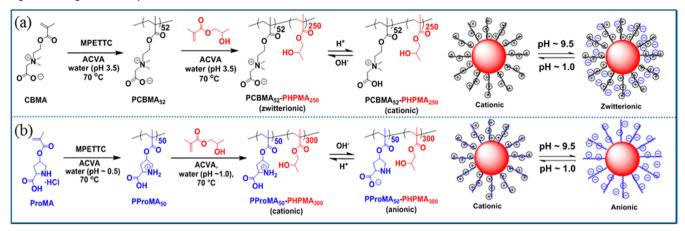[†]Department of Chemistry, University of Sheffield, Brook Hill, Sheffield, South Yorkshire S3 7HF, United Kingdom
[‡]The School of Materials, University of Manchester, Oxford Road, Manchester, M13 9PL, United Kingdom
[§]School of Chemistry, University of Leeds, Woodhouse Lane, Leeds LS2 9JT, United Kingdom
[∥]Department of Polymer Chemistry, Kyoto University, Kyoto 615-8510, Japan

S *Supporting Information*

ABSTRACT: New spherical diblock copolymer nanoparticles were synthesized via RAFT aqueous dispersion polymerization of 2-hydroxypropyl methacrylate (HPMA) at 70 °C and 20% w/w solids using either poly(carboxybetaine methacrylate) or poly(proline methacrylate) as the steric stabilizer block. Both of these stabilizers contain carboxylic acid groups, but poly(proline methacrylate) is anionic above pH 9.2, whereas poly(carboxybetaine methacrylate) has zwitterionic character at this pH. When calcite crystals are grown at an initial pH of 9.5 in the presence of these two types of nanoparticles, it is found that the anionic poly(proline methacrylate)-stabilized particles are occluded uniformly throughout the crystals (up to 6.8% by mass, 14.0% by volume). In contrast, the zwitterionic poly(carboxybetaine methacrylate)-stabilized particles show no signs of occlusion into calcite crystals grown under identical conditions. The presence of carboxylic acid groups alone therefore does not guarantee efficient occlusion: overall anionic character is an additional prerequisite.

The occlusion of water-soluble organic molecules into inorganic crystals has been intensely studied in order to modify crystal morphologies, understand occlusion mechanisms, and achieve enhanced mechanical properties such as toughness.[1−11] Recently, it has been shown that various nanoparticles ranging from 20 to 250 nm diameter can be incorporated within calcite crystals grown from aqueous solution via the ammonium carbonate diffusion method.[12−15] Nanoparticle occlusion within the host crystal has been confirmed by electron microscopy studies.[12−17] The resulting nanocomposite crystals can exhibit greater hardness compared to calcite of geological origin.[12,13] Based on studies to date, it seems that carboxylate functionality at the nanoparticle surface promotes efficient occlusion within calcite. However, the design rules for occlusion are not yet understood. This lack of detailed molecular level understanding is a significant barrier to optimizing the occlusion efficiency for calcite and also for extending occlusion to include alternative inorganic host crystals. Ultimately, this is the key to producing new copolymer/crystal nanocomposites that exhibit a range of tailored properties. In the present study, we examine the "carboxylate surface functionality" design rule in more detail.

The synthesis of bespoke organic nanoparticles of controllable size, shape, and surface chemistry is a formidable technical challenge.[12,18−20] However, we and others have shown that reversible addition−fragmentation chain-transfer (RAFT)-mediated polymerization-induced self-assembly (PISA) provides a versatile and efficient route for the synthesis of diblock copolymer spheres, worms, or vesicles.[21−25] In particular, PISA syntheses can be conducted in concentrated aqueous solution,[26−40] and the size and morphology of the resulting diblock copolymer nano-objects can be readily adjusted by systematically varying the DP of the core-forming hydrophobic block.[26,41] Moreover, the surface chemistry of such nano-objects can be readily controlled by using nonionic,[26,42−44] anionic,[45,46] cationic,[47,48] or zwitterionic[49−51] blocks as the steric stabilizer for the PISA formulation.

Here, RAFT-mediated PISA is used to design two new examples of amphiphilic diblock copolymer nanoparticles. More specifically, either a poly(carboxybetaine methacrylate) (PCBMA$_{52}$) macromolecular chain transfer agent (macro-CTA) or a poly(proline methacrylate) (PProMA$_{50}$) macro-CTA is chain-extended with 2-hydroxypropyl methacrylate (HPMA) via RAFT aqueous dispersion polymerization at 70 °C and 20% w/w solids. In both cases, the stabilizer block contains carboxylate groups. However, PProMA$_{50}$ is *anionic* above pH 9.2, whereas PCBMA$_{52}$ possesses *zwitterionic* character (see Scheme 1). Thus, the design rule hypothesis

Scheme 1. Synthesis of (a) PCBMA$_{52}$-PHPMA$_{250}$ and (b) PProMA$_{50}$-PHPMA$_{300}$ Diblock Copolymer Nanoparticles via RAFT Aqueous Dispersion Polymerization of HPMA at 70 °C[a]

[a]The cartoons depict the surface charge on these two types of sterically-stabilized nanoparticles at approximately pH 1.0 and pH 9.5, respectively.
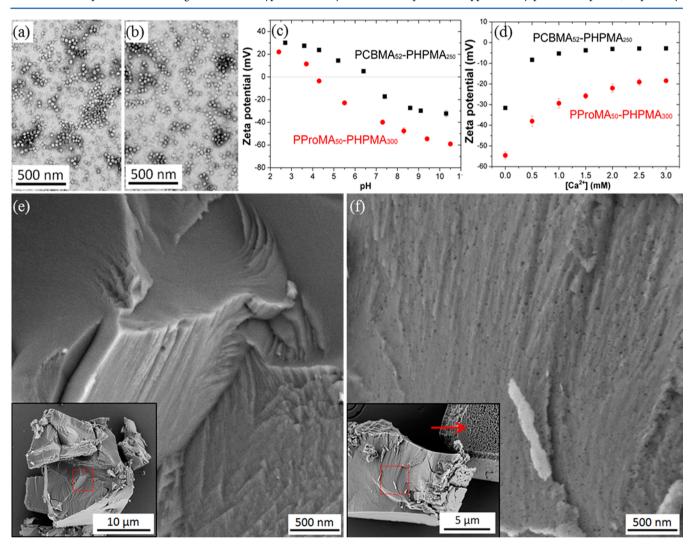

Figure 1. TEM images recorded for (a) PCBMA$_{52}$-PHPMA$_{250}$ and (b) PProMA$_{50}$-PHPMA$_{300}$ diblock copolymer nanoparticles; (c) zeta potential vs pH and (d) zeta potential vs [Ca^{2+}] obtained at pH 9.5 for PCBMA$_{52}$-PHPMA$_{250}$ and PProMA$_{50}$-PHPMA$_{300}$ nanoparticles; SEM images showing cross-sections of calcium carbonate crystals precipitated in the presence of 0.01% w/w of (e) PCBMA$_{52}$-PHPMA$_{250}$ and (f) PProMA$_{50}$-PHPMA$_{300}$ nanoparticles. The insets show low magnification images of the same crystals with dashed red squares indicating the areas shown in (e) and (f). The red arrow indicates the rough surface of the calcite. Clearly, there is no nanoparticle occlusion in (e), whereas there is extensive occlusion in (f).

that will be tested herein is the following: *is the presence of carboxylate groups alone sufficient to promote efficient nanoparticle occlusion within calcite or is overall anionic character also required?*

Base titration of the carboxylic acid group in CBMA monomer indicated a pK_a of ~2.3 (see Figure S1a, Supporting Information). The quaternary ammonium group in CBMA confers permanent cationic charge, so this molecule becomes zwitterionic after deprotonation of its carboxylic acid group (see Scheme 1a).[52−54] O-Methacryloyl-trans-4-hydroxy-L-proline (ProMA) was synthesized according to a literature protocol (see Scheme S1, Supporting Information).[55] This monomer exhibits two pK_a values (pK_{a1} = 1.5, pK_{a2} = 9.0, see Figure S1b) owing to its secondary amine and carboxylic acid groups. PCBMA$_{52}$ and PProMA$_{50}$ were synthesized via RAFT polymerization in aqueous solution (Scheme 1). This was achieved using a water-soluble (below pH 4.5) trithiocarbonate-based RAFT CTA (MPETTC) containing a morpholine group, which was prepared via a two-step synthesis as recently described by Penfold and co-workers (see Scheme S2).[56] Kinetic studies of the RAFT homopolymerization of CBMA and ProMA using MPETTC at 70 °C confirmed that high conversions (>90%) were obtained within 3 h and there was a linear evolution of molecular weight with conversion in each case, as expected for well-controlled RAFT polymerizations (see Figures S2 and S3). Aqueous GPC studies indicated relatively low polydispersities (M_w/M_n < 1.2) for both PCBMA$_{52}$ and PProMA$_{50}$ macro-CTAs. Self-blocking experiments were conducted by addition of a further charge of the corresponding monomer (i.e., CBMA to the PCBMA$_{52}$ macro-CTA or ProMA to the PProMA$_{50}$ macro-CTA). In both cases a relatively high blocking efficiency was achieved, suggesting that the majority of trithiocarbonate RAFT chain-ends remained intact (see Figure S4).

Sterically-stabilized diblock copolymer nanoparticles were readily synthesized by chain extension of each macro-CTA in turn with HPMA using a RAFT aqueous dispersion polymerization formulation. PCBMA$_{52}$ macro-CTA and PProMA$_{50}$ macro-CTA have similar degrees of polymerization, so the stabilizer layer thicknesses of the resulting copolymer nanoparticles are comparable. PCBMA$_{52}$-PHPMA$_{250}$ and PProMA$_{50}$-PHPMA$_{300}$ were targeted since preliminary experiments indicated that such diblock copolymer compositions gave almost identical mean particle diameters. Indeed, transmission electron microscopy (TEM) analysis indicated that both types of nanoparticles possessed narrow particle size distributions with a mean diameter of 34.5 ± 3.4 nm for PCBMA$_{52}$-PHPMA$_{250}$ and 33.6 ± 4.4 nm for PProMA$_{50}$-PHPMA$_{300}$. Dynamic light scattering studies confirmed that both types of nanoparticles exhibited essentially unchanged hydrodynamic diameters in the absence and presence of 1.5 mM [Ca^{2+}], which indicated good colloidal stability under the conditions typically used for calcium carbonate formation (see Figure S5).[12−15] Aqueous electrophoresis measurements revealed that both types of nanoparticles were cationic at low pH but became anionic at high pH, with PCBMA$_{52}$-PHPMA$_{250}$ and PProMA$_{50}$-PHPMA$_{300}$ exhibiting isoelectric points (IEPs) at around pH 6.6 and 4.1, respectively (Figure 1c). The effect of addition of [Ca^{2+}] on nanoparticle zeta potential was also examined at pH 9.5 (Figure 1d). In both cases, the initial highly anionic character observed in the absence of any salt was significantly reduced, suggesting extensive Ca^{2+} binding to the steric stabilizer chains. However, the PProMA$_{50}$-PHPMA$_{300}$ nano-

particles retained a relatively high net negative zeta potential of −25 mV at [Ca^{2+}] = 1.5 mM, whereas the zeta potential for the PCBMA$_{52}$-PHPMA$_{250}$ was reduced to just −3 mV under the same conditions. This difference appears to be decisive in dictating the nanoparticle occlusion efficiency in each case (see later).

Calcium carbonate crystals were precipitated at an initial pH of 9.5 by exposing an aqueous solution of 1.5 mM [Ca^{2+}] containing 0.01% w/w PCBMA$_{52}$-PHPMA$_{250}$ or PProMA$_{50}$-PHPMA$_{300}$ nanoparticles to ammonium carbonate vapor at 20 °C for 24 h. As expected, experiments conducted in the absence of any nanoparticles, or in the presence of *non-ionic* nanoparticles, resulted in the formation of 30−50 μm rhombohedral crystals, which is typically characteristic of calcite (see Figures S6 and S7). Similarly, precipitation in the presence of the PCBMA$_{52}$-PHPMA$_{250}$ nanoparticles also yielded rhombohedral morphology, but with a minor population of a second crystal phase (see Figures S8a and S8b). Crystals grown in the presence of PProMA$_{50}$-PHPMA$_{300}$ nanoparticles were also rhombohedral but had smaller dimensions of 10−30 μm (see Figures S8c and S8d).

The internal crystal morphology was evaluated by examining cross-sections of deliberately fractured crystals. There was no evidence of any nanoparticle occlusion within crystals grown in the presence of PCBMA$_{52}$-PHPMA$_{250}$ nanoparticles (Figure 1e). However, when PProMA$_{50}$-PHPMA$_{300}$ nanoparticles were used as an additive, the crystals had roughened surfaces and some truncation of the edges was observed, as indicated in the inset of Figure 1f. SEM images of the internal crystal structure confirmed that PProMA$_{50}$-PHPMA$_{300}$ nanoparticles were uniformly distributed throughout the whole crystal (Figure 1f). Further, the apparent voids/occluded nanoparticles were comparable in diameter to the PProMA$_{50}$-PHPMA$_{300}$ nanoparticles prior to occlusion.
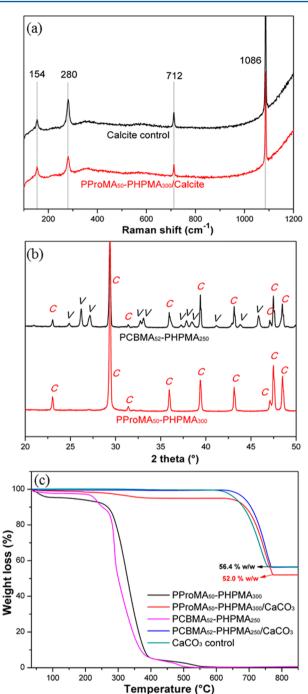
Raman spectroscopy studies (Figure 2a) indicated that crystals containing PProMA$_{50}$-PHPMA$_{300}$ nanoparticles possessed various spectral features that are known to be characteristic of calcite; bands at 154 and 280 cm^{-1} are lattice modes, while bands at 712 cm^{-1} (v_4) and 1086 cm^{-1} (v_1) have been assigned to the in-plane bending and symmetric stretching of carbonate, respectively.[57,58] Bulk crystal structures were confirmed by powder XRD studies (Figure 2b). In particular, calcium carbonate precipitated in the presence of PCBMA$_{52}$-PHPMA$_{250}$ nanoparticles results in a mixture of calcite and vaterite phases. This is probably because the PCBMA$_{52}$-PHPMA$_{250}$ nanoparticles can act as an "impurity" that slightly perturbs normal calcite growth. In contrast, only calcite was detected for calcium carbonate prepared in the presence of PProMA$_{50}$-PHPMA$_{300}$ nanoparticles.

Thermogravimetric analysis (TGA; Figure 2c) studies confirmed that there was no detectable occlusion of PCBMA$_{52}$-PHPMA$_{250}$ while the calcite/PProMA$_{50}$-PHPMA$_{300}$ crystals comprised 6.8% w/w nanoparticles. Assuming a copolymer density of 1.22 g cm^{-3}, this corresponds to 14% v/v (see calculation in the Supporting Information). Nanoparticle occlusion was further confirmed by FT-IR spectroscopy (see Figure S9).

Previously, we reported that anionic nanoparticles containing surface carboxylate groups could be occluded within calcite.[12−15] Furthermore, it was suggested that this motif played a key role in promoting occlusion. In the present study, both PCBMA$_{52}$-PHPMA$_{250}$ and PProMA$_{50}$-PHPMA$_{300}$ nanoparticles also possess surface carboxylate groups. However, the

Figure 2. (a) Raman spectra recorded for a calcite crystal control and calcite containing occluded PProMA$_{50}$-PHPMA$_{300}$ nanoparticles; (b) XRD patterns recorded for calcite precipitated in the presence of PCBMA$_{52}$-PHPMA$_{250}$ (*C* denotes calcite and *V* denotes vaterite) and PProMA$_{50}$-PHPMA$_{300}$; (c) TGA curves recorded for PProMA$_{50}$-PHPMA$_{300}$ and PCBMA$_{52}$-PHPMA$_{250}$ nanoparticles alone, calcite crystals grown in the presence of either PCBMA$_{52}$-PHPMA$_{250}$ or PProMA$_{50}$-PHPMA$_{300}$, and a pure calcite control.

former *zwitterionic* nanoparticles exhibit no signs of occlusion, while the overall *anionic* PProMA$_{50}$-PHPMA$_{300}$ copolymer nanoparticles are homogeneously incorporated into calcite crystals at approximately 6.8% w/w. These observations indicate that both the presence of carboxylic acid groups *and* the overall anionic character are required for successful nanoparticle occlusion.

A reasonable explanation for these observations is as follows. Ca^{2+} ions interact strongly with the anionic carboxylate groups on both the zwitterionic PCBMA$_{52}$ and the anionic PProMA$_{50}$ stabilizer chains at pH 9.5. However, the overall zeta potential is reduced to around −3 mV in the presence of 1.5 mM [Ca^{2+}] in the former case (Figure 1d), which is insufficient to ensure strong electrostatic adsorption of the PCBMA$_{52}$-PHPMA$_{250}$ nanoparticles onto the growing crystal surface.[4] In contrast, PProMA$_{50}$-PHPMA$_{300}$ nanoparticles retain an anionic zeta potential of −25 mV under the same conditions, which enables their strong electrostatic binding onto the growing crystal surface.[13,14,59] Thus, the subtle structural differences between these two types of sterically-stabilized nanoparticles has a dramatic effect on their interactions with growing calcite crystals.

In summary, this study demonstrates that surface carboxylate functionality is a necessary but not sufficient condition for efficient nanoparticle occlusion within calcite. Overall *anionic* character appears to be an additional prerequisite, because essentially no occlusion is observed when *zwitterionic* polycarboxybetaine-stabilized nanoparticles are employed. This work provides a deeper understanding of the design rules for efficient nanoparticle occlusion within this particular inorganic host crystal.

■ ASSOCIATED CONTENT

ⓈSupporting Information

The Supporting Information is available free of charge on the ACS Publications website at DOI: 10.1021/acsmacro-lett.6b00022.

> Experimental details, reaction schemes for the synthesis of the MPETTC RAFT agent and ProMA monomer, titration data, GPC data, DLS, optical micrographs, SEM images, and FT-IR spectra (PDF).

■ AUTHOR INFORMATION

Corresponding Author
*E-mail: s.p.armes@sheffield.ac.uk.

Notes
The authors declare no competing financial interest.

■ ACKNOWLEDGMENTS

■ REFERENCES

(1) Teng, H. H.; Dove, P. M.; Orme, C. A.; De Yoreo, J. J. *Science* **1998**, *282*, 724−727.
(2) Li, H.; Xin, H. L.; Muller, D. A.; Estroff, L. A. *Science* **2009**, *326*, 1244−1247.
(3) Yu, S. H.; Cölfen, H. *J. Mater. Chem.* **2004**, *14*, 2124−2147.
(4) Metzler, R. A.; Tribello, G. A.; Parrinello, M.; Gilbert, P. U. P. A. *J. Am. Chem. Soc.* **2010**, *132*, 11585−11591.
(5) Meldrum, F. C.; Cölfen, H. *Chem. Rev.* **2008**, *108*, 4332−4432.
(6) Naka, K.; Chujo, Y. *Chem. Mater.* **2001**, *13*, 3245−3259.
(7) Estroff, L. A.; Hamilton, A. D. *Chem. Mater.* **2001**, *13*, 3227−3235.

(8) Alves, N. M.; Leonor, I. B.; Azevedo, H. S.; Reis, R. L.; Mano, J. F. *J. Mater. Chem.* **2010**, *20*, 2911−2921.

(9) Pokroy, B.; Kapon, M.; Marin, F.; Adir, N.; Zolotoyabko, E. *Proc. Natl. Acad. Sci. U.S.A.* **2007**, *104*, 7337−7341.

(10) Pokroy, B.; Fitch, A.; Zolotoyabko, E. *Adv. Mater.* **2006**, *18*, 2363−2368.

(11) De Yoreo, J. J.; Gilbert, P. U. P. A.; Sommerdijk, N. A. J. M.; Penn, R. L.; Whitelam, S.; Joester, D.; Zhang, H.; Rimer, J. D.; Navrotsky, A.; Banfield, J. F.; Wallace, A. F.; Michel, F. M.; Meldrum, F. C.; Cölfen, H.; Dove, P. M. *Science* **2015**, *349*, 6760.

(12) Kim, Y.-Y.; Ribeiro, L.; Maillot, F.; Ward, O.; Eichhorn, S. J.; Meldrum, F. C. *Adv. Mater.* **2010**, *22*, 2082−2086.

(13) Kim, Y.-Y.; Ganesan, K.; Yang, P.; Kulak, A. N.; Borukhin, S.; Pechook, S.; Ribeiro, L.; Kroeger, R.; Eichhorn, S. J.; Armes, S. P.; Pokroy, B.; Meldrum, F. C. *Nat. Mater.* **2011**, *10*, 890−896.

(14) Kulak, A. N.; Semsarilar, M.; Kim, Y.-Y.; Ihli, J.; Fielding, L. A.; Cespedes, O.; Armes, S. P.; Meldrum, F. C. *Chem. Sci.* **2014**, *5*, 738−743.

(15) Kulak, A. N.; Yang, P.; Kim, Y.-Y.; Armes, S. P.; Meldrum, F. C. *Chem. Commun.* **2014**, *50*, 67−69.

(16) Hanisch, A.; Yang, P.; Kulak, A. N.; Fielding, L. A.; Meldrum, F. C.; Armes, S. P. *Macromolecules* **2016**, *49*, 192−204.

(17) Kim, Y.-Y.; Semsarilar, M.; Carloni, J. D.; Cho, K. R.; Kulak, A. N.; Polishchuk, I.; Hendley, C. T.; Smeets, P. J. M.; Fielding, L. A.; Pokroy, B.; Tang, C. C.; Estroff, L. A.; Baker, S. P.; Armes, S. P.; Meldrum, F. C. *Adv. Funct. Mater.* **2016**, DOI: 10.1002/adfm.201504292.

(18) Muñoz-Espí, R.; Qi, Y.; Lieberwirth, I.; Gómez, C. M.; Wegner, G. *Chem. - Eur. J.* **2006**, *12*, 118−129.

(19) Li, C.; Qi, L. *Angew. Chem., Int. Ed.* **2008**, *47*, 2388−2393.

(20) Lu, C. H.; Qi, L. M.; Cong, H. L.; Wang, X. Y.; Yang, J. H.; Yang, L. L.; Zhang, D. Y.; Ma, J. M.; Cao, W. X. *Chem. Mater.* **2005**, *17*, 5218−5224.

(21) Blanazs, A.; Armes, S. P.; Ryan, A. J. *Macromol. Rapid Commun.* **2009**, *30*, 267−277.

(22) Warren, N. J.; Armes, S. P. *J. Am. Chem. Soc.* **2014**, *136*, 10174−10185.

(23) Derry, M. J.; Fielding, L. A.; Armes, S. P. *Prog. Polym. Sci.* **2016**, *52*, 1−18.

(24) Sun, J.-T.; Hong, C.-Y.; Pan, C.-Y. *Polym. Chem.* **2013**, *4*, 873−881.

(25) Cunningham, M. F. *Prog. Polym. Sci.* **2008**, *33*, 365−398.

(26) Li, Y.; Armes, S. P. *Angew. Chem., Int. Ed.* **2010**, *49*, 4042−4046.

(27) Warren, N. J.; Mykhaylyk, O. O.; Ryan, A. J.; Williams, M.; Doussineau, T.; Dugourd, P.; Antoine, R.; Portale, G.; Armes, S. P. *J. Am. Chem. Soc.* **2015**, *137*, 1929−1937.

(28) Warren, N. J.; Mykhaylyk, O. O.; Mahmood, D.; Ryan, A. J.; Armes, S. P. *J. Am. Chem. Soc.* **2014**, *136*, 1023−1033.

(29) Tan, J.; Sun, H.; Yu, M.; Sumerlin, B. S.; Zhang, L. *ACS Macro Lett.* **2015**, *4*, 1249−1253.

(30) Yu, Q.; Ding, Y.; Cao, H.; Lu, X.; Cai, Y. *ACS Macro Lett.* **2015**, *4*, 1293−1296.

(31) Chaduc, I.; Crepet, A.; Boyron, O.; Charleux, B.; D'Agosto, F.; Lansalot, M. *Macromolecules* **2013**, *46*, 6013−6023.

(32) An, Z.; Shi, Q.; Tang, W.; Tsung, C.-K.; Hawker, C. J.; Stucky, G. D. *J. Am. Chem. Soc.* **2007**, *129*, 14493−14499.

(33) Sumerlin, B. S.; Lowe, A. B.; Thomas, D. B.; McCormick, C. L. *Macromolecules* **2003**, *36*, 5982−5987.

(34) Mitsukami, Y.; Donovan, M. S.; Lowe, A. B.; McCormick, C. L. *Macromolecules* **2001**, *34*, 2248−2256.

(35) Zhang, W.; D'Agosto, F.; Boyron, O.; Rieger, J.; Charleux, B. *Macromolecules* **2011**, *44*, 7584−7593.

(36) Boisse, S.; Rieger, J.; Belal, K.; Di-Cicco, A.; Beaunier, P.; Li, M.-H.; Charleux, B. *Chem. Commun.* **2010**, *46*, 1950−1952.

(37) Mable, C. J.; Gibson, R. R.; Prévost, S.; McKenzie, B. E.; Mykhaylyk, O. O.; Armes, S. P. *J. Am. Chem. Soc.* **2015**, *137*, 16098−16108.

(38) Jia, Z.; Bobrin, V. A.; Truong, N. P.; Gillard, M.; Monteiro, M. J. *J. Am. Chem. Soc.* **2014**, *136*, 5824−5827.

(39) Ferguson, C. J.; Hughes, R. J.; Nguyen, D.; Pham, B. T. T.; Gilbert, R. G.; Serelis, A. K.; Such, C. H.; Hawkett, B. S. *Macromolecules* **2005**, *38*, 2191−2204.

(40) Zhou, W.; Qu, Q.; Xu, Y.; An, Z. *ACS Macro Lett.* **2015**, *4*, 495−499.

(41) Cunningham, V. J.; Alswieleh, A. M.; Thompson, K. L.; Williams, M.; Leggett, G. J.; Armes, S. P.; Musa, O. M. *Macromolecules* **2014**, *47*, 5613−5623.

(42) Blanazs, A.; Verber, R.; Mykhaylyk, O. O.; Ryan, A. J.; Heath, J. Z.; Douglas, C. W. I.; Armes, S. P. *J. Am. Chem. Soc.* **2012**, *134*, 9741−9748.

(43) Blanazs, A.; Ryan, A. J.; Armes, S. P. *Macromolecules* **2012**, *45*, 5099−5107.

(44) Blanazs, A.; Madsen, J.; Battaglia, G.; Ryan, A. J.; Armes, S. P. *J. Am. Chem. Soc.* **2011**, *133*, 16581−16587.

(45) Semsarilar, M.; Ladmiral, V.; Blanazs, A.; Armes, S. P. *Langmuir* **2012**, *28*, 914−922.

(46) Semsarilar, M.; Jones, E. R.; Blanazs, A.; Armes, S. P. *Adv. Mater.* **2012**, *24*, 3378−3382.

(47) Semsarilar, M.; Ladmiral, V.; Blanazs, A.; Armes, S. P. *Langmuir* **2013**, *29*, 7416−7424.

(48) Smith, A. E.; Xu, X.; Kirkland-York, S. E.; Savin, D. A.; McCormick, C. L. *Macromolecules* **2010**, *43*, 1210−1217.

(49) Doncom, K. E. B.; Warren, N. J.; Armes, S. P. *Polym. Chem.* **2015**, *6*, 7264−7273.

(50) Sugihara, S.; Blanazs, A.; Armes, S. P.; Ryan, A. J.; Lewis, A. L. *J. Am. Chem. Soc.* **2011**, *133*, 15707−15713.

(51) Sun, J.-T.; Yu, Z.-Q.; Hong, C.-Y.; Pan, C.-Y. *Macromol. Rapid Commun.* **2012**, *33*, 811−818.

(52) Kharlampieva, E.; Izumrudov, V. A.; Sukhishvili, S. A. *Macromolecules* **2007**, *40*, 3663−3668.

(53) Matsuoka, H.; Yamakawa, Y.; Ghosh, A.; Saruwatari, Y. *Langmuir* **2015**, *31*, 4827−4836.

(54) Kitano, H.; Tokuwa, K.-i.; Ueno, H.; Li, L.; Saruwatari, Y. *Colloid Polym. Sci.* **2015**, *293*, 2931−2939.

(55) Kristensen, T. E.; Vestli, K.; Fredriksen, K. A.; Hansen, F. K.; Hansen, T. *Org. Lett.* **2009**, *11*, 2968−2971.

(56) Penfold, N. J. W.; Lovett, J. R.; Warren, N. J.; Verstraete, P.; Smets, J.; Armes, S. P. *Polym. Chem.* **2016**, *7*, 79−88.

(57) Wehrmeister, U.; Soldati, A. L.; Jacob, D. E.; Haeger, T.; Hofmeister, W. *J. Raman Spectrosc.* **2010**, *41*, 193−201.

(58) Ihli, J.; Bots, P.; Kulak, A.; Benning, L. G.; Meldrum, F. C. *Adv. Funct. Mater.* **2013**, *23*, 1965−1973.

(59) Cho, K.-R.; K, Y.-Y.; Yang, P.; Cai, W.; Pan, H.; Kulak, A. N.; Lau, J. L.; Kulshreshtha, P.; Armes, S. P.; Meldrum, F. C.; De Yoreo, J. J. *Nat. Commun.* **2016**, *7*, 10187.